736 *Biochemistry* **2010,** *49,* 736–741
DOI: 10.1021/bi9018412

BIOCHEMISTRY
including biophysical chemistry & molecular biology
Article

Direct Observation of the pH-Dependent Equilibrium between Metarhodopsins I and II and the pH-Independent Interaction of Metarhodopsin II with Transducin C-Terminal Peptide†

Keita Sato, Takefumi Morizumi,‡ Takahiro Yamashita, and Yoshinori Shichida*

Department of Biophysics, Graduate School of Science, Kyoto University, Kyoto 606-8502, Japan.
‡Present address: Institut für Medizinische Physik and Biophysik, Charité Universitätsmedizin Berlin, Berlin, Germany.

Received October 27, 2009; Revised Manuscript Received December 18, 2009

ABSTRACT: Bovine rhodopsin contains 11-*cis*-retinal as a light-absorbing chromophore that binds to a lysine residue of the apoprotein opsin via a protonated Schiff base linkage. Light isomerizes 11-*cis*-retinal into the all-trans form, which eventually leads to the formation of an enzymatically active state, metarhodopsin II (MII). It is widely believed that MII forms a pH-dependent equilibrium with metarhodopsin I (MI), but direct evidence for this equilibrium has not been reported. Here, we confirmed this equilibrium by direct observation of the mutual conversions of MI and MII upon changing the pH of the MI/MII mixture. We also observed a reversible binding of the synthetic peptide constituting the C-terminal 11 amino acids of the transducin α-subunit to MII, which resulted in change of the amounts of MI and MII in the equilibrium. Interestingly, addition of the peptide did not induce a simple pK_a shift but rather induced an increase of the MII fraction at high pH. These results indicate that in addition to the MII that is formed from MI in a pH-dependent manner there also exists another MII, which is in equilibrium with MI in a pH-independent manner and can bind to the peptide. Therefore, there is no need for proton uptake by the protein moiety of opsin for the binding to the peptide.

Rhodopsin is the photoreceptor protein present in rod photoreceptor cells of the vertebrate retina and a member of family A of G protein-coupled receptors (GPCRs).[1] It consists of a protein moiety, opsin, and a chromophore, 11-*cis*-retinal. Opsin is folded into a characteristic seven transmembrane α-helical structure, and the chromophore covalently binds to opsin's lysine residue at position 296 of helix VII via a protonated Schiff base linkage (*1*). Light isomerizes the 11-*cis*-retinal chromophore to the highly twisted all-trans form in a restricted cavity in opsin (*2*). The highly twisted chromophore then induces stepwise changes of opsin's structure, finally resulting in the formation of metarhodopsin II (MII). MII contains deprotonated Schiff base chromophore (*3*) and is the enzymatically active state responsible for G protein activation (*4*). Because the proton on the Schiff base mediates the ionic lock between the chromophore and a counterion, Glu113 (*5*−*7*), its transfer to the counterion results in the loss of the lock (*8*), which enables the conformation near the Schiff base to be more flexible. It has frequently been suggested that this deprotonation of the Schiff base of MII plays a role in forming a stable complex with G protein and inducing its GDP−GTP exchange reaction (*9*).

To achieve a full understanding of the G protein activation mechanism of MII, it is of primary importance to elucidate the mechanism of the formation of MII. MII is formed as a mixture with metarhodopsin I (MI), which contains a protonated Schiff base chromophore (*3*). It has been reported that the ratio between MI and MII in the sample is dependent on the temperature, pH, and other environmental conditions (*10*−*12*). Thus it is generally thought that MI and MII are in temperature- and pH-dependent equilibrium. However, in most experiments reported thus far, rhodopsin samples kept at various temperatures or pHs were irradiated to form a mixture of MI and MII, and the formation of the mixtures was analyzed by a reaction scheme that included MI/MII equilibrium. Thus, the possibility that precursors of MI and MII could form an equilibrium and then be converted to MI and MII, which exhibit no equilibrium (Scheme 1), could not be neglected. Direct evidence for the existence of the state of equilibrium between MI and MII should be obtained from the observation of the temperature- or pH-driven reverse reaction from either of the intermediates. However, accurate control of the sample temperature and pH is necessary to avoid the inclusion of reactions such as decomposition into all-*trans*-retinal and opsin and conversion to the subsequent intermediate metarhodopsin III (MIII) in the measurements of reverse reactions.

Using low-temperature time-resolved spectroscopy, we previously tried to directly observe the thermal back-reaction from MII to MI and confirmed that MI, MII, and even lumirhodopsin are actually in a temperature-dependent equilibrium (*13*). However, as far as we know, no experimental data explicitly showing the pH-driven reverse reactions have been published so far. Thus, in the present study, using a specialized optical cell with two

†This work was supported in part by Grants-in-Aid for Scientific Research and the Global Center of Excellence Program (A06) from the Japanese Ministry of Education, Culture, Sports, Science, and Technology to Y.S. K.S. was supported by a JSPS Research Fellowship for Young Scientists.

*To whom correspondence should be addressed. Telephone: +81-75-753-4213. Fax: +81-75-753-4210. E-mail: shichida@rh.biophys.kyoto-u.ac.jp.

[1]Abbreviations: GPCR, G protein-coupled receptor; MI, metarhodopsin I; MII, metarhodopsin II; ROS, rod outer segment; PC, L-α-phosphatidylcholine from egg yolk; CHAPS, 3-[(3-cholamidopropyl)dimethylammonio]-propanesulfonate; Tris, tris(hydroxymethyl)aminomethane; HEPES, 2-[4-(2-hydroxyethyl)-1-piperazinyl]ethanesulfonic acid; DTT, dithiothreitol; ConA, concanavalin A; GtαCT, 11-mer synthetic peptide corresponding to the C-terminus of the transducin α-subunit; HAA, 11-mer high-affinity synthetic peptide analogous to the C-terminus of the transducin α-subunit.

 Published on Web 12/23/2009

Scheme 1

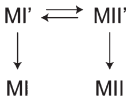

compartments, we examined whether or not the spectra of the samples whose pH was adjusted to the same value before and after irradiation were overlapping. The results clearly showed that these spectra were identical, indicating that MI and MII are really in pH-dependent equilibrium. Furthermore, we observed that a synthetic peptide composed of the C-terminal 11 amino acids of the transducin α-subunit reversibly changed the amounts of MI and MII in the mixture. Examination of the pH profile of the MI/MII mixture indicated that the peptide did not simply bind to MII, but rather, in addition to the MII that forms from MI in a pH-dependent manner, there was also present another MII that formed an equilibrium with MI in a pH-independent manner and could bind to the peptide. On the basis of these experimental results, we discuss the mechanism of activation of G protein by rhodopsin.

MATERIALS AND METHODS

Sample Preparation. Bovine rod outer segments (ROS) were isolated from bovine retinas by a standard discontinuous sucrose gradient method described previously (*14*). To remove peripheral proteins associated with ROS, the ROS were treated with 5 M urea followed by repeated washing (five times) with a low ionic strength buffer [5 mM Tris, 0.5 mM $MgCl_2$, 1 mM DTT, 0.8 μg/mL leupeptin, 10 KIU/mL aprotinin, pH 7.2 (at 20 °C)]. The ROS thus obtained were subjected to the experiments. Purified rhodopsin was prepared as described previously (*15*). That is, ROS were solubilized in buffer E [0.6% (w/v) CHAPS, 0.8 mg/mL PC, 140 mM NaCl, 3 mM $MgCl_2$, 50 mM HEPES, 1 mM DTT, pH 7.5 (at 20 °C)] and applied to a ConA−Sepharose column, from which rhodopsin was eluted with buffer E containing 0.3 M methyl α-D-mannopyranoside. The ROS and the purified rhodopsin samples were stored at −80 °C until use. An 11-mer synthetic peptide at the C-terminus of the transducin α-subunit (GtαCT, NH_2-IKENLKDCGLF-COOH) and its high-affinity analogue (HAA, NH_2-VLEDLKSCGLF-COOH) (*16*) were purchased from Kurabo Co. Ltd.

Spectrophotometry. Absorption spectra were recorded using a Shimadzu UV2400 spectrophotometer. An optical cell having two compartments, each with a 0.437 cm path length (Starna), was used for rapidly changing the pH of the sample or swift addition of the transducin-derived peptide into the sample after irradiation of the sample under temperature-controlled conditions. An optical cell with one compartment (width, 2 mm; light path, 1 cm) was also used for the conventional recording of the spectra of the samples. To control the sample temperature, an optical cell holder was connected to a Neslab RTE-7 temperature controller. Accordingly, the sample temperature was kept at 0 ± 0.1 °C. The sample was irradiated with light from a 1 kW tungsten halogen lamp (Rigaku Seiki) that had been passed through a glass cutoff filter (VO57; Toshiba).

The amount of rhodopsin photoconverted to the intermediates by the irradiation was estimated as follows: First, hydroxylamine was added to the irradiated sample at a final concentration of 50 mM, followed by incubation at 25 °C until intermediates present in the sample were completely converted to retinal oxime and the opsin. Then the sample was cooled to 0 °C, and the spectrum was recorded. Subsequently, the sample was reirradiated with yellow light (> 500 nm light) at 25 °C to bleach the residual rhodopsin present in the sample, and the spectrum was recorded at 0 °C. The percentage of the residual rhodopsin present in the irradiated sample was estimated by comparing the peak value (500 nm) of the difference spectrum between these spectra with that of the original rhodopsin sample. Judging from the shape of the difference spectrum, isorhodopsin which might have been produced from MI photoreaction was negligible under our experimental conditions.

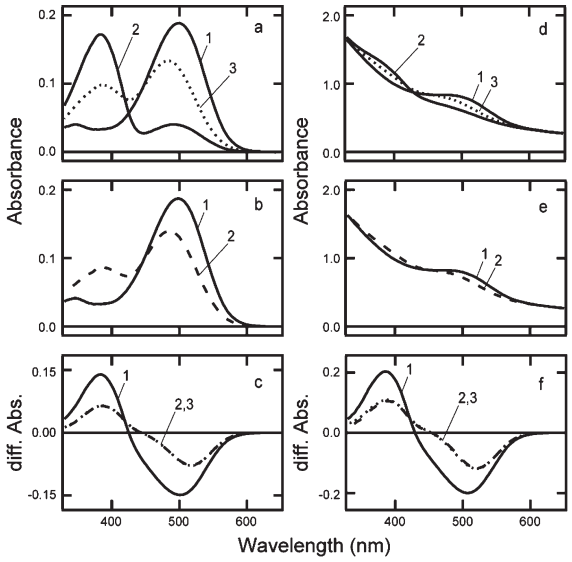

FIGURE 1: Direct observation of the conversion of MII to MI upon changing the pH of the MI/MII mixture. All of the spectra were recorded at 0 °C. (a) Curves 1 and 2 are the spectra of CHAPS-solubilized rhodopsin and its photoproduct produced by irradiation of rhodopsin with > 550 nm light for 30 s at pH 5.2. Curve 3 is the spectrum of the photoproduct after changing the pH to 7.2. (b) Curves 1 and 2 are the spectra of CHAPS-solubilized rhodopsin and its photoproduct produced by irradiation of rhodopsin with > 550 nm light for 30 s at pH 7.2. (c) Curve 1 is the difference spectrum calculated by subtracting curve 1 from curve 2 in (a). Curve 2 is the spectrum calculated by subtracting curve 1 from curve 3 in (a). Curve 3 is the spectrum calculated by subtracting the curve 1 from curve 2 in (b). (d) Curves 1 and 2 are the spectra of rhodopsin in ROS and its photoproduct produced by irradiation of rhodopsin with > 550 nm light for 30 s at pH 6.1. Curve 3 is the spectrum of the photoproduct after changing the pH to 7.1. (e) Curves 1 and 2 are the spectra of rhodopsin in ROS and its photoproduct produced by irradiation of rhodopsin with > 550 nm light for 30 s at pH 7.1. (f) Curve 1 is the difference spectrum calculated by subtracting curve 1 from curve 2 in (d). Curve 2 is the spectrum calculated by subtracting curve 1 from curve 3 in (d). Curve 3 is the spectrum calculated by subtracting curve 1 from curve 2 in (f).

RESULTS

Direct Observation of a pH-Dependent MI/MII Equilibrium. We measured the absorption spectra of bovine rhodopsin samples, the pH of which was adjusted to 7.2 before and after irradiation. To make a quick and accurate change of pH in the sample after irradiation, we used an optical cell with two separate compartments. In one experiment, the detergent-purified rhodopsin sample (pH 5.2) was placed into one compartment of the optical cell, and the same volume of buffer solution was placed into the other compartment. After the spectrum was recorded (curve 1 in Figure 1a), rhodopsin in the sample was irradiated with > 550 nm light for 30 s to convert it to a mixture of MI and MII. Under these conditions, mainly MII was formed

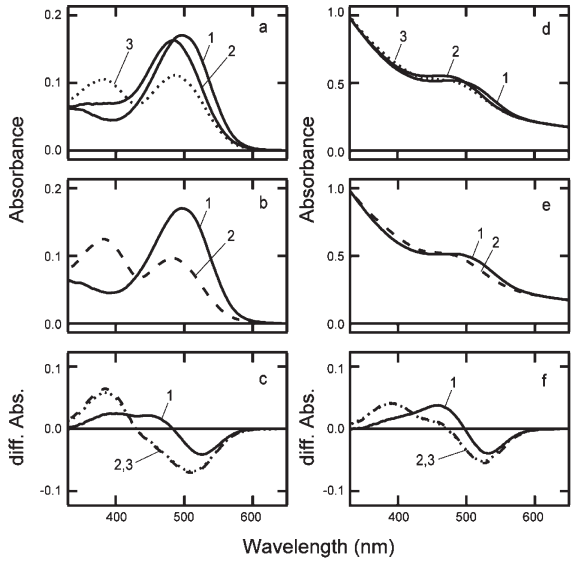

FIGURE 2: Direct observation of the conversion of MI to MII upon changing the pH of the MI/MII mixture. All of the spectra were recorded at 0 °C. (a) Curves 1 and 2 are the spectra of CHAPS-solubilized rhodopsin and its photoproduct produced by irradiation of rhodopsin with >550 nm light for 30 s at pH 7.8. Curve 3 is the spectrum of the photoproduct after changing the pH to 6.7. (b) Curves 1 and 2 are the spectra of CHAPS-solubilized rhodopsin and its photoproduct produced by irradiation of rhodopsin with >550 nm light for 30 s at pH 6.7. (c) Curve 1 is the difference spectrum calculated by subtracting curve 1 from curve 2 in (a). Curve 2 is the spectrum calculated by subtracting curve 1 from curve 3 in (a). Curve 3 is the spectrum calculated by subtracting curve 1 from curve 2 in (b). (d) Curves 1 and 2 are the spectra of rhodopsin in ROS and its photoproduct produced by irradiation of rhodopsin with >550 nm light for 30 s at pH 8.7. Curve 3 is the spectrum of the photoproduct after changing the pH to 7.3. (e) Curves 1 and 2 are the spectra of rhodopsin in ROS and its photoproduct produced by irradiation of rhodopsin with >550 nm light for 30 s at pH 7.3. (f) Curve 1 is the difference spectrum calculated by subtracting curve 1 from curve 2 in (d). Curve 2 is the spectrum calculated by subtracting curve 1 from curve 3 in (d). Curve 3 is the spectrum calculated by subtracting curve 1 from curve 2 in (f).

(curve 2 in Figure 1a). The irradiated rhodopsin sample was then mixed with the buffer solution of the other compartment by inversion of the optical cell. This manipulation raised the pH of the sample to 7.2 and changed the spectrum in a manner that indicated an increase of MI component in the sample (curve 3 in Figure 1a). In the other experiment, the rhodopsin sample (pH 5.2) and the buffer in the respective compartments of the optical cell were first mixed by inverting the cell. The spectrum of the mixture (pH 7.2, curve 1 in Figure 1b) was identical with that of the rhodopsin sample before mixing with the buffer (curve 1 in Figure 1a). The sample was then irradiated with >550 nm light for 30 s, resulting in the formation of a mixture containing mainly MI (curve 2 in Figure 1b).

The difference spectrum calculated by subtracting curve 1 from curve 3 in Figure 1a was compared with that calculated by subtracting curve 1 from curve 2 in Figure 1b (Figure 1c). These two spectra overlapped perfectly with each other, indicating that MII in the pH 5.2 sample was indeed converted to MI when the pH of the sample was raised to 7.2. We also performed similar experiments using ROS samples. The results (Figure 1d−f) clearly showed that the conversion of MII to MI by raising the pH also occurred in the membrane-embedded condition.

Figure 2 shows a series of experiments in which the pHs of CHAPS-solubilized rhodopsin (pH 7.8) and rhodopsin in ROS

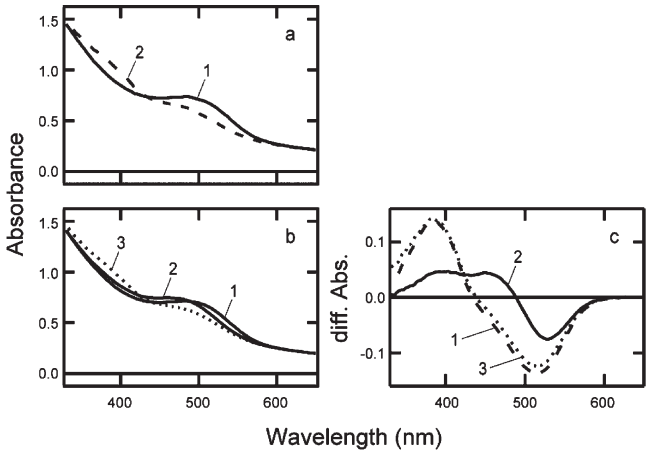

FIGURE 3: Effect of the high-affinity synthetic peptide on the equilibrium between MI and MII. All of the spectra were recorded at 0 °C. (a) Curves 1 and 2 are the spectra of rhodopsin in ROS (pH 7.5) in the presence of the high-affinity synthetic peptide (HAA; final concentration 20 μM) and its photoproduct produced by irradiation of rhodopsin with >550 nm light for 30 s. (b) Curves 1 and 2 are the spectra of rhodopsin in ROS and its photoproduct produced by irradiation of rhodopsin with >550 nm light for 30 s. Curve 3 is the spectrum after addition of the high-affinity synthetic peptide (HAA; final concentration 20 μM) obtained by using a special optical cell with two compartments. (c) Curve 1 is the difference spectrum calculated by subtracting curve 1 from curve 2 in (a). Curve 2 is the spectrum calculated by subtracting curve 1 from curve 2 in (b). Curve 3 is the spectrum calculated by subtracting curve 1 from curve 3 in (b).

(pH 8.7) samples were lowered to 6.7 and 7.3 by mixing with the buffer, respectively. The fact that the difference spectra were overlapped (Figure 2c,f) clearly showed that MI formed under alkaline conditions can be converted to MII upon lowering the pH. All of these results clearly showed that MI and MII can be interconvertible depending on the pH environment; that is, MI and MII are in a direct pH-dependent equilibrium. This is the first direct and clear evidence for the complete equilibrium of these intermediates.

Effect of Synthetic Peptide on the MI/MII equilibrium. It has been reported that irradiation of rhodopsin in the presence of transducin or the C-terminal peptide of the transducin α-subunit causes the formation of a larger amount of MII than expected based on the pH of the sample. Thus, next we examined whether intermediates present in the equilibrium mixture, but not their precursors, bind to the peptide. First, we prepared a rhodopsin sample containing the C-terminal peptide (curve 1 in Figure 3a) and irradiated it with >550 nm light for 30 s (curve 2 in Figure 3a). Then, using the optical cell with two compartments, we irradiated a rhodopsin sample containing no peptide and then added the peptide into the rhodopsin sample. The difference spectrum calculated by subtracting the spectrum recorded after addition of the peptide from that before irradiation has almost the same shape as that calculated from the spectra of the peptide-containing rhodopsin sample before and after irradiation. These data imply that the peptide can bind directly to the intermediates in the equilibrium mixture. We also demonstrated that reduction of the peptide concentration by dilution with buffer causes the loss of MII formation (data not shown), indicating that the mode of interaction of the peptide with MII is reversible. It should be noted that the difference spectrum calculated by subtracting curve 2 from curve 3 in Figure 3c has the same shape as that calculated by subtracting curve 1 from curve 2 in Figure 2c, indicating that the binding of the peptide to MII does not affect the absorption characteristics of MII.

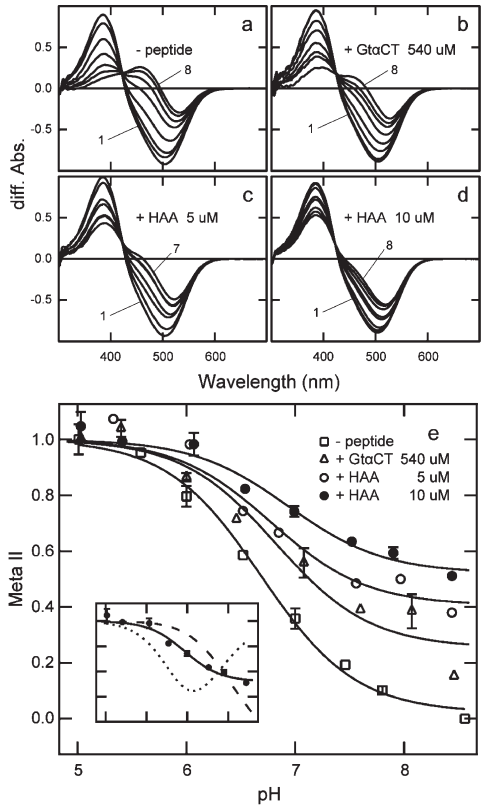

FIGURE 4: pH-dependent shift of the equilibrium between MI and MII in the presence or absence of synthetic peptides. All of the spectra were recorded at 0 °C. (a) A set of difference spectra between rhodopsin in ROS and its irradiation photoproduct at pH 5.0, 5.6, 6.1, 6.5, 7.1, 7.5, 8.0, and 8.6 (curves 1−8, respectively). (b) A set of difference spectra between rhodopsin in ROS and its irradiation photoproduct in the presence of 540 mM GtαCT at pH 5.0, 5.4, 6.0, 6.5, 7.1, 7.6, 8.1, and 8.5 (curves 1−8, respectively). (c) A set of difference spectra between rhodopsin in ROS and its irradiation photoproduct in the presence of 5 mM HAA at pH 5.3, 6.0, 6.5, 6.9, 7.6, 8.0, and 8.4 (curves 1−7, respectively). (d) A set of difference spectra between rhodopsin in ROS and its irradiation photoproduct in the presence of 10 mM HAA at pH 5.0, 5.4, 6.1, 6.5, 7.0, 7.5, 7.9, and 8.4 (curves 1−8, respectively). The amount of bleached rhodopsin in (a)−(d) was 5.85 ± 0.42 μM. All of the difference spectra in (a)−(d) were normalized so that the absorbance of bleached rhodopsin was 1. (e) Relative amounts of MII as a function of pH. The amounts of MII produced by irradiation of rhodopsin in ROS with > 550 nm light for 30 s at various pHs in the absence of the peptides (squares) and the presence of 540 μM GtαCT (triangles), 5 μM HAA (open circles), or 10 μM HAA (closed circles) were plotted as a function of pH of the sample. The amount of MII was estimated by simulating each difference spectrum with absorption spectra of MII and MI, which were obtained by the method previously reported (*15*). Solid lines are the best-fitted curves calculated according to Scheme 3. The equilibrium constants K_1 and K_2 were estimated to be 2.24×10^{-2} and 2.22×10^{8} M^{-1}, respectively, by best-fitting of the experimental data in the absence of peptide according to the Scheme 2, and these values were used for the fitting of the data in the presence of peptides according to the Scheme 3. Inset: The experimental data obtained in the presence of 10 μM HAA are shown in closed circles, which are best-fitted according to Scheme 3 (solid line). The broken and dotted lines are the best-fitted curves calculated from Schemes 4 and 5, respectively. Note that K_3 was fixed at 1 in fitting based on Scheme 5 because Knierim et al. (*23*) reported that maximum net proton release from MII is 0.5 proton per MII in the presence of peptide.

pH Profile of the MI/MII Equilibrium in the Presence of Peptide. Using ROS samples, we next examined the pH profile of the MI/MII equilibrium in the presence of peptide to obtain insight into the mechanism of interaction between the rhodopsin intermediate and the peptide. We used two kinds of peptides: one was a peptide consisting of the C-terminal 11 amino acids of Gtα and the other was its high-affinity analogue developed by Martin et al. (*16*). If the peptide can bind to MII to affect the MI/MII equilibrium, the presence of peptide would shift the apparent pK_a of the MI/MII equilibrium. However, the experimental results clearly showed that addition of the peptide increased the MII fraction at high pH instead of a simple shift of pK_a (Figure 4). In particular, the addition of high-affinity peptide at 10 μM concentration resulted in the presence of ~60% of MII in the equilibrium mixture even at pH 8.5, in which MII constituted only a few percent of the total intermediates in the absence of peptide. We also performed experiments using CHAPS-solubilized rhodopsin samples and obtained results similar to those shown in Figure 4 (data not shown).

Scheme 2

Scheme 3

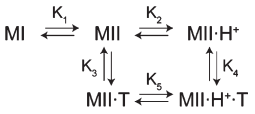

Scheme 4

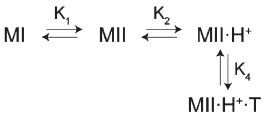

The above results suggested that the equilibrium state contains at least two kinds of MII: one is an MII that forms an equilibrium with MI independent of the environmental pH, and the other is an MII that receives one proton from the outer environment. We tentatively referred them to as MII and MII·H^+ and formulated a reaction scheme according to these plus the previously published results (Scheme 2) (*17*). Then we formulated two schemes in which interaction modes with peptide were differently included (Schemes 3 and 4). In Schemes 3 and 4, we assumed that both of MII (MII and MII·H^+) and only MII·H^+ have binding affinities to the peptide, respectively. The relative amount of MII was calculated based on these schemes (see Appendix), and experimental data were fitted with the theoretical curves (Figure 4e). The obtained data could be fitted with the curves calculated from Scheme 3 better than with the curves from Scheme 4. It should be noted that the binding of peptide to MII·H^+ was necessary for better fitting.

It is important to verify whether or not the K values obtained from Scheme 3 are in agreement with the experimental facts reported previously. It was reported that HAA has 100-fold higher affinity to the active state than GtαCT (*16*). The K_3 and K_4 values we obtained are 2.64×10^{-2} μM^{-1} and 1.50×10^{-3} μM^{-1} in the presence of 540 μM GtαCT, 1.09×10 μM^{-1} and 4.76×10^{-1} μM^{-1} in the presence of 5 μM HAA, and 6.80 μM^{-1} and 4.37×10^{-1} μM^{-1} in the presence of 10 μM HAA, respectively. Thus K_3 and K_4 values in the presence of HAA were 200−300-fold higher than those in the presence of GtαCT, which is consistent with the previous report. Interestingly, our data indicated that each K_3 value is 10-fold larger than K_4 value. This indicates that MII has 10-fold higher affinity to transducin-derived peptide than MII·H^+.

Scheme 5

$$\mathrm{MI} \overset{K_1}{\rightleftharpoons} \mathrm{MII{\cdot}H^+} \overset{K_2}{\rightleftharpoons} \mathrm{MII{\cdot}T} \overset{K_3}{\rightleftharpoons} \mathrm{MII{\cdot}(\text{-}H^+){\cdot}T}$$

DISCUSSION

In the present study, we have confirmed the pH equilibrium between MI and MII by directly measuring their mutual conversions. We also found a reversible effect of the C-terminal peptide of Gtα on the MI/MII equilibrium and obtained the pH profile of the MI/MII equilibrium in the presence of the peptide. The results showed that addition of peptide did not simply shift the pK_a of the MI/MII equilibrium but, rather, increased the amount of MII at high pH without a large shift of pK_a. The experimental data were best fitted with a reaction scheme (Scheme 3) in which the peptide can interact with MII that has not yet acquired a proton from the solution environment.

Normally, proton dissociable groups bind protons at lower pH and release them at higher pH. Although MI and MII contain protonated and unprotonated Schiff base chromophores, respectively, the shift of the equilibrium occurs in the opposite compared to the normal way: that is, higher pH shifts the equilibrium in favor of MI and lower pH shifts it in favor of MII (*10*). These facts suggest that there is a dissociable residue in the protein region accessible to the solution environment and it controls the state of Schiff base protonation through an intramolecular hydrogen-bonding network. Although the molecular entities constituting the hydrogen-bonding network have not been identified yet, mutational studies have shown that Glu134 is a candidate for the acceptor of a proton from the solution environment (*19*). This was also strengthened by the FTIR experiments (*18*, *20*).

In the present study, we showed that MII could interact with the peptide without proton uptake. Therefore, the proton uptake by Glu134 is not essential for binding to transducin but, rather, is important for the release of GDP or uptake of GTP. In fact, we reported that there is an intermediate state that can bind GDP-bound transducin but cannot induce the GDP−GTP exchange reaction (*21*, *22*). All of these data taken together indicate that the MII state without proton uptake seems to bind transducin that has already released GDP (empty state).

When we constructed the reaction schemes, we assumed that the peptide could simply interact with MII states. However, recent investigations by Knierim et al. (*23*) suggested that more than one proton is released from the MII state when rhodopsin binds to the peptide. Thus, we also tried to simulate the experimental data by using a reaction scheme involving the proton release from the MII−peptide complex (Scheme 5). According to this reaction scheme, it is expected that the amount of MII would first decrease as the pH of the sample is raised but would then increase if the pH goes up further. However, the experimental data did not show a reincrease of the amount of MII at higher pH, indicating that proton release from the MII−peptide complex did not occur under our experimental conditions. It should be noted that our experimental data are well fitted with the assumption that only one proton is released from the MII−peptide complex. In this scenario, the peptide can interact with MII that has already acquired a proton.

In contrast to the vertebrate rhodopsins, invertebrate rhodopsins contain a metarhodopsin system whose Schiff bases are directly affected by the solution environment (*24*). This is in marked contrast with the fact that, like vertebrate rhodopsins, most invertebrate rhodopsins have a conserved carboxylic residue at the cytoplasmic surface. These observations can be accounted for by the fact for that the hydrogen-bonding network system including E113 does not exist in invertebrate rhodopsins (*25*, *26*). These differences may reflect the small helical rearrangements and thus less efficient G protein activation in the case of invertebrate rhodopsin upon photon absorption (*27*, *28*). It seems likely that vertebrate rhodopsins acquired their anomalous pH-dependent property of metarhodopsins during evolution.

In conclusion, we obtained direct evidence that MI and MII form a pH-dependent equilibrium. We also obtained evidence that proton uptake by MII is not necessary for interaction with transducin. In our next study, we will attempt to identify the amino acid residues involved in the hydrogen-bonding network system connecting Glu134 with the Schiff base chromophore.

ACKNOWLEDGMENT

We thank Dr. Y. Imamoto for valuable discussions and Dr. E. Nakajima for critical reading of the manuscript and invaluable comments.

APPENDIX

To analyze the pH dependence of MI and MII in the absence and presence of transducin-derived peptides, we considered the reaction schemes (Schemes 2, 3, and 4) shown in the Results section. In Scheme 2, the total amount of bleached rhodopsin [Rh] is given by

$$[\mathrm{Rh}] = [\mathrm{MI}] + [\mathrm{MII}] + [\mathrm{MII{\cdot}H^+}] \tag{1}$$

where [MI], [MII], and [MII·H^+] are the amounts of MI, MII, and MII·H^+. From the law of mass action, the right side can be written as

$$[\mathrm{Rh}] = [\mathrm{MI}]([1 + K_1 + K_1K_2[\mathrm{H^+}]) \tag{2}$$

where K_1 and K_2 are the MI/MII and MII/ MII·H^+ equilibrium constants, respectively, and [H^+] is the proton concentration in the sample. The amount of MI is given by

$$[\mathrm{MI}] = \frac{[\mathrm{Rh}]}{1 + K_1 + K_1K_2[\mathrm{H^+}]} \tag{3}$$

Therefore, the relative amount of MII is derived to be

$$[\mathrm{MII}]_{\mathrm{rel}} = \frac{[\mathrm{MII}] + [\mathrm{MII{\cdot}H^+}]}{[\mathrm{Rh}]} = 1 - \frac{[\mathrm{MI}]}{[\mathrm{Rh}]}$$

$$= 1 - \frac{1}{1 + K_1 + K_1K_2[\mathrm{H^+}]} \tag{4}$$

In Scheme 3, the total amount of bleached rhodopsin is given by

$$[\mathrm{Rh}] = [\mathrm{MI}] + [\mathrm{MII}] + [\mathrm{MII{\cdot}H^+}] + [\mathrm{MII{\cdot}T}] + [\mathrm{MII{\cdot}H^+{\cdot}T}] \tag{5}$$

where [MII·T] and [MII·H^+·T] are the amounts of MII·T and MII·H^+·T. From the law of mass action, the right side can be written as

$$[\mathrm{Rh}] = [\mathrm{MI}](1 + K_1 + K_1K_2[\mathrm{H^+}] + K_1K_3[\mathrm{T}] + K_1K_2K_4[\mathrm{H^+}][\mathrm{T}]) \tag{6}$$

where [T] is the amount of transducin-derived peptide. On the other, the total amount of transducin-derived peptide is given by

$$[T]_{total} = [T] + [MII\cdot T] + [MII\cdot H^+\cdot T] \quad (7)$$

Hence, the amount of free peptide can be expressed as

$$[T] = \frac{[T]_{total}}{1 + K_1K_3[T] + K_1K_2K_4[H^+][T]} \quad (8)$$

Substituting eq 8 into eq 6, we obtain

$$0 = [MI]^2K_aK_b + [MI](K_a + K_b([T]_{total} - [Rh])) - [Rh] \quad (9)$$

where K_a and K_b are expressed as

$$K_a = 1 + K_1 + K_1K_2[H^+] \quad (10)$$

and

$$K_b = K_1K_3 + K_1K_2K_4[H^+] \quad (11)$$

K_3 and K_4 are the MII/MII·T and MII·H^+/MII·H^+·T equilibrium constants, respectively. K_a and K_b are functions of pH. By solving the quadratic equation (eq 9) for [MI], the amount of MI is given by

$$[MI] = \{-(K_a + K_b([T]_{total} - [Rh])) + \sqrt{(K_a + K_b([T]_{total} - [Rh]))^2 + 4K_aK_b[Rh]}\}/2K_aK_b \quad (12)$$

Finally, the amount of MII is obtained by the equation:

$$[MII]_{rel} = 1 - \frac{[MI]}{[Rh]} = 1 - \{-(K_a + K_b([T]_{total} - [Rh])) + \sqrt{(K_a + K_b([T]_{total} - [Rh]))^2 + 4K_aK_b[Rh]}\}/2K_aK_b[Rh] \quad (13)$$

We used eqs 4 and 13 for analyzing the experimental data. If K_3 is fixed as 0, eq 13 derives the relative amount of MII in Scheme 4.

REFERENCES

1. Palczewski, K., Kumasaka, T., Hori, T., Behnke, C. A., Motoshima, H., Fox, B. A., Le Trong, I., Teller, D. C., Okada, T., Stenkamp, R. E., Yamamoto, M., and Miyano, M. (2000) Crystal structure of rhodopsin: A G protein-coupled receptor. *Science 289*, 739–745.
2. Kandori, H., Shichida, Y., and Yoshizawa, T. (2001) Photoisomerization in rhodopsin. *Biochemistry* (*Moscow*) *66*, 1197–1209.
3. Doukas, A. G., Aton, B., Callender, R. H., and Ebrey, T. G. (1978) Resonance Raman studies of bovine metarhodopsin I and metarhodopsin II. *Biochemistry 17*, 2430–2435.
4. Hofmann, K. P. (1985) Effect of GTP on the rhodopsin-G-protein complex by transient formation of extra metarhodopsin II. *Biochim. Biophys. Acta 810*, 278–281.
5. Sakmar, T. P., Franke, R. R., and Khorana, H. G. (1989) Glutamic acid-113 serves as the retinylidene Schiff base counterion in bovine rhodopsin. *Proc. Natl. Acad. Sci. U.S.A. 86*, 8309–8313.
6. Zhukovsky, E. A., and Oprian, D. D. (1989) Effect of carboxylic acid side chains on the absorption maximum of visual pigments. *Science 246*, 928–930.
7. Nathans, J. (1990) Determinants of visual pigment absorbance: identification of the retinylidene Schiff's base counterion in bovine rhodopsin. *Biochemistry 29*, 9746–9752.
8. Jäger, F., Fahmy, K., Sakmar, T. P., and Siebert, F. (1994) Identification of glutamic acid 113 as the Schiff base proton acceptor in the metarhodopsin II photointermediate of rhodopsin. *Biochemistry 33*, 10878–10882.
9. Emeis, D., Kühn, H., Reichert, J., and Hofmann, K. P. (1982) Complex formation between metarhodopsin II and GTP-binding protein in bovine photoreceptor membranes leads to a shift of the photoproduct equilibrium. *FEBS Lett. 143*, 29–34.
10. Matthews, R. G., Hubbard, R., Brown, P. K., and Wald, G. (1963) Tautomeric forms of metarhodopsin. *J. Gen. Physiol. 47*, 215–240.
11. Parkes, J. H., and Liebman, P. A. (1984) Temperature and pH dependence of the metarhodopsin I−metarhodopsin II kinetics and equilibria in bovine rod disk membrane suspensions. *Biochemistry 23*, 5054–5061.
12. Mitchell, D. C., and Litman, B. J. (2000) Effect of ethanol and osmotic stress on receptor conformation. Reduced water activity amplifies the effect of ethanol on metarhodopsin II formation. *J. Biol. Chem. 275*, 5355–5360.
13. Imai, H., Mizukami, T., Imamoto, Y., and Shichida, Y. (1994) Direct observation of the thermal equilibria among lumirhodopsin, metarhodopsin I, and metarhodopsin II in chicken rhodopsin. *Biochemistry 33*, 14351–14358.
14. Morizumi, T., Imai, H., and Shichida, Y. (2003) Two-step mechanism of interaction of rhodopsin intermediates with the C-terminal region of the transducin alpha-subunit. *J. Biochem. 134*, 259–267.
15. Morizumi, T., Imai, H., and Shichida, Y. (2005) Direct observation of the complex formation of GDP-bound transducin with the rhodopsin intermediate having a visible absorption maximum in rod outer segment membranes. *Biochemistry 44*, 9936–9943.
16. Martin, E. L., Rens-Domiano, S., Schatz, P. J., and Hamm, H. E. (1996) Potent peptide analogues of a G protein receptor-binding region obtained with a combinatorial library. *J. Biol. Chem. 271*, 361–366.
17. Arnis, S., and Hofmann, K. P. (1993) Two different forms of metarhodopsin II: Schiff base deprotonation precedes proton uptake and signaling state. *Proc. Natl. Acad. Sci. U.S.A. 90*, 7849–7853.
18. Fahmy, K., Sakmar, T. P., and Siebert, F. (2000) Transducin-dependent protonation of glutamic acid 134 in rhodopsin. *Biochemistry 39*, 10607–10612.
19. Arnis, S., Fahmy, K., Hofmann, K. P., and Sakmar, T. P. (1994) A conserved carboxylic acid group mediates light-dependent proton uptake and signaling by rhodopsin. *J. Biol. Chem. 269*, 23879–23881.
20. Vogel, R., Mahalingam, M., Lüdeke, S., Huber, T., Siebert, F., and Sakmar, T. P. (2008) Functional role of the "ionic lock"—an interhelical hydrogen-bond network in family A heptahelical receptors. *J. Mol. Biol. 380*, 648–655.
21. Tachibanaki, S., Imai, H., Mizukami, T., Okada, T., Imamoto, Y., Matsuda, T., Fukada, Y., Terakita, A., and Shichida, Y. (1997) Presence of two rhodopsin intermediates responsible for transducin activation. *Biochemistry 36*, 14173–14180.
22. Tachibanaki, S., Imai, H., Terakita, A., and Shichida, Y. (1998) Identification of a new intermediate state that binds but not activates transducin in the bleaching process of bovine rhodopsin. *FEBS Lett. 425*, 126–130.
23. Knierim, B., Hofmann, K. P., Ernst, O. P., and Hubbell, W. L. (2007) Sequence of late molecular events in the activation of rhodopsin. *Proc. Natl. Acad. Sci. U.S.A. 104*, 20290–20295.
24. Hubbard, R., and St. George, R. C. (1958) The rhodopsin system of the squid. *J. Gen. Physiol. 41*, 501–528.
25. Okada, T., Fujiyoshi, Y., Silow, M., Navarro, J., Landau, E. M., and Shichida, Y. (2002) Functional role of internal water molecules in rhodopsin revealed by X-ray crystallography. *Proc. Natl. Acad. Sci. U.S.A. 99*, 5982–5987.
26. Murakami, M., and Kouyama, T. (2008) Crystal structure of squid rhodopsin. *Nature 453*, 363–367.
27. Tsukamoto, H., Farrens, D. L., Koyanagi, M., and Terakita, A. (2009) The magnitude of the light-induced conformational change in different rhodopsins correlates with their ability to activate G proteins. *J. Biol. Chem. 284*, 20676–20683.
28. Terakita, A., Koyanagi, M., Tsukamoto, H., Yamashita, T., Miyata, T., and Shichida, Y. (2004) Counterion displacement in the molecular evolution of the rhodopsin family. *Nat. Struct. Mol. Biol. 11*, 284–289.